EASTERN SECTION
SEISMOLOGICAL
RESEARCH LETTERS

# The Canadian Rockies and Alberta Network (CRANE): New Constraints on the Rockies and Western Canada Sedimentary Basin

**Yu Jeffrey Gu, Ahmet Okeler, Luyi Shen, and Sean Contenti**
**Department of Physics, University of Alberta**

## ABSTRACT

The Canadian Rockies and the neighboring Alberta Basin mark the transition from the old North American continental lithosphere (east) to young accreted "terranes" (west). Geologic, seismic, and magnetic data in this region have suggested complex crustal domains, conductive anomalies, and major seismic velocity gradients in the mantle. However, the nature of the boundaries between the basement domains and their vertical extents remains controversial due to the lack of exposed geology and limited seismic and electromagnetic receivers. Since 2006, the seismic data coverage and depth sensitivity have received a major boost from the establishment of the Canadian Rockies and Alberta Network (nicknamed CRANE), the first semi-permanent broadband seismic array in Alberta. The availability of the array data provides vital constraints on the regional micro-earthquakes and crust/mantle seismic structures. Among the broad range of ongoing efforts, this study highlights promising results from the analyses of *P*-to-*S* wave receiver functions, shear wave splitting amplitudes/directions, and ambient seismic noise. Our preliminary receiver-function stacks show that the base of the crust gradually shallows from approximately 60 km beneath the Rockies near the Canadian-U.S. border to 37–40 km beneath central Alberta; the latter range is consistent with earlier findings from active-source experiments. Converted waves from "littered" crust and/or lithosphere have also been detected at a number of stations in the depth range of 80–130 km. Complexities in the lithosphere are further evidenced by our regional shear wave splitting measurements. We infer a strong east-west change of mantle flow pattern, consistent with present-day plate motion. The spatial distribution of the *SKS* fast orientations highlights the contrasting crust/mantle structures and histories between the Rockies and adjacent domains. Dynamic effects associated with a migrating continental root east of the province may be important. Finally, our preliminary inversions using ambient seismic noise indicate more than 0.8 km/s in peak-to-peak group velocity variations throughout the crust. The upper crust beneath the Alberta Basin is dominated by low Rayleigh-wave group velocities. A lower-than-expected correlation between seismic velocities and tectonic domain boundaries suggests significant tectonic overprinting in the southern Western Canada Sedimentary Basin. Overall, the broadband seismic data from CRANE could play a key role in uncovering the mysteries of the crust and mantle beneath the transition region between cratons and terranes.

## INTRODUCTION

The emergence of three-component, broadband seismic networks in recent years has accelerated the progress in seismic monitoring and structural imaging. Equipped with digital instruments sensitive to a wide frequency band (0.01–100 Hz), earthquake seismologists no longer need to contend with analog records or inaccurate readings from microfiche machines. The exceptional global data quality and coverage from dense temporary/permanent deployments, such as USArray (continental United States) and Hi-net/J-Array (Japan), have overcome many conceptual and practical barriers in global seismological data analysis. Consequently, the global seismology community can now take greater advantage of methods predicated upon superior data density and distribution (see Gu 2010 for reviews).

Canada has traditionally been at the forefront of this era of improved seismic monitoring and imaging. The success of the Lithoprobe project, a trans-Canada experiment initiated in 1995, marked a milestone in multiscale, multidisciplinary research efforts. Continuously evolving array

doi: 10.1785/gssrl.82.4.575

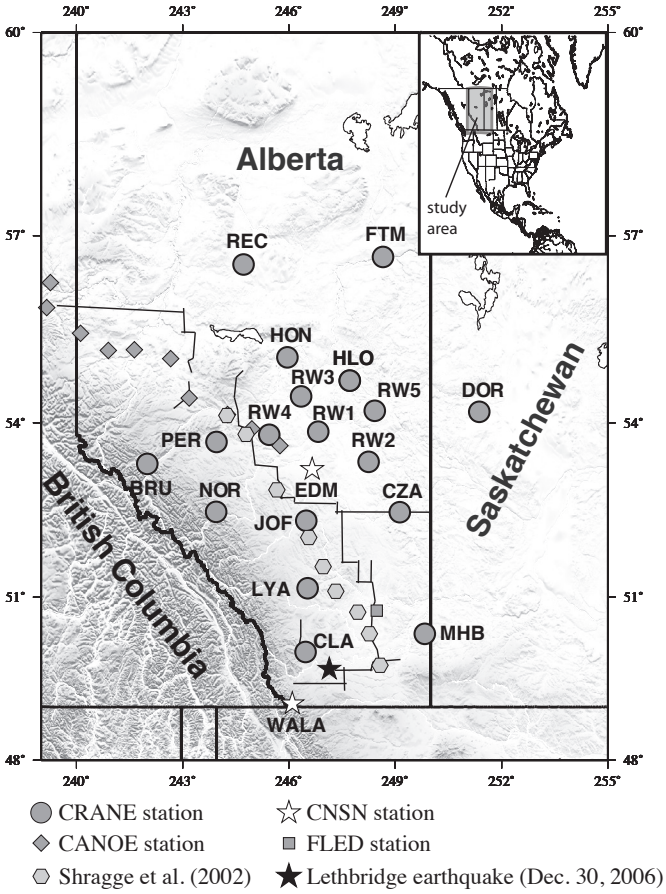


▲ **Figure 1.** Distribution of CRANE, Canadian National Seismic Network (CNSN), and other temporary stations in Alberta. Also shown are active source reflection/refraction lines from the Lithoprobe project and a local *Mb* = 3.5 earthquake that took place on December 30, 2006. The map inset shows the geographical location of the study area in relation to the North American continent. Station FTM was upgraded and renamed FMC shortly after the initial deployment.

experiments in Yellowknife, British Columbia, and Hudson Bay have also been crucial in mapping regional seismicity and crust/mantle structure under North America. Unfortunately, the data coverage within inland provinces such as Alberta, Saskatchewan, and Manitoba remains spotty. Most of the seismic experiments prior to 2005, *e.g.*, Lithoprobe, Florida to Edmonton Broadband Seismometer Experiment (FLED), and the Canadian Northwest Experiment (CANOE) (Figure 1), adopted linear receiver geometries that considerably undersampled the southern part of the Western Canada Sedimentary Basin (WCSB).

Since early 2006 the regional seismic data coverage has been significantly improved by the establishment of CRANE, the first semi-permanent broadband seismic array in Alberta and parts of Saskatchewan, Canada. Continuous seismic signals from this array show great promise in resolving the details of regional seismicity and crust/mantle structures. Important inferences can be made, despite the early stage of the data analysis, regarding the tectonic history and dynamics of the

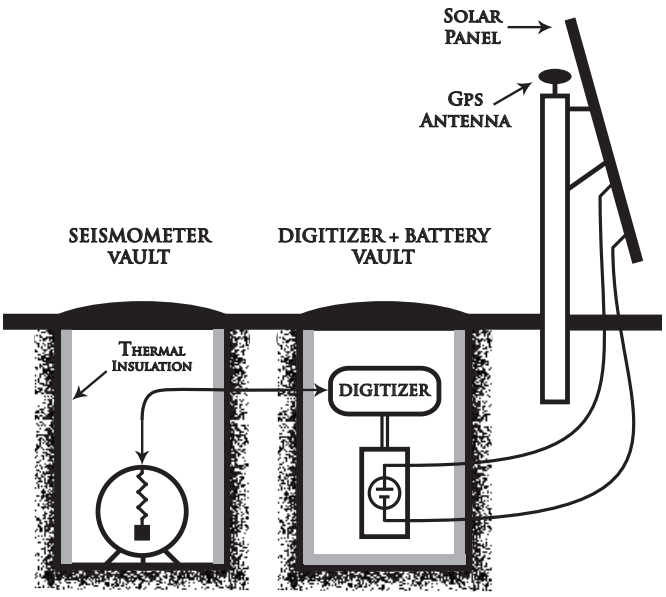


▲ **Figure 2.** A schematic diagram of the instrument setup at a typical CRANE station. Seismometers and digitizers are housed in different underground vaults powered by a solar panel and a rechargeable 12V battery.

northern Rockies and WCSB. This study aims to provide an overview of the array and some of the early findings based on the data collected during the past three years.

## ARRAY SETUP AND SEISMIC DATA ACQUISITION

The deployment of CRANE stations began in late 2005 under the funding support of the Canadian Foundation for Innovation (CFI) and the University of Alberta. Six broadband seismic instruments were initially acquired and installed in central and southern Alberta, mostly on private land relatively removed from cultural and industrial noise. The array has since been expanded to 18 stations and presently forms a semi-uniform grid with an average station spacing of ~150 km (see Figure 1). Site selections were made based on 1) distance from the two operational permanent Canadian National Seismic Network (CNSN) stations EDM and WALA in Alberta, 2) local topography and soil characteristics, 3) all-season road access and security, and finally 4) level of cultural noise associated with traffic and power lines.

The majority of the CRANE stations are equipped with three-component (east-west, north-south, and vertical) Trillium 240 and 120 seismometers (manufactured by Nanometrics Inc.) with relatively flat responses between corner frequencies of 0.005–0.01 Hz (low) and 100+ Hz (high). Each seismometer is connected to a digitizer (Taurus, Nanometrics Inc.) (Figure 2) where the sample rate is generally set at 20 Hz. Seismometers and digitizers are housed within separate underground vaults, powered by 30–80 W solar panels connected to 12V rechargeable batteries; see Figure 2 for a schematic diagram of this self-sustaining system. These ~1.5-m-deep vaults are sealed and well insulated to 1)

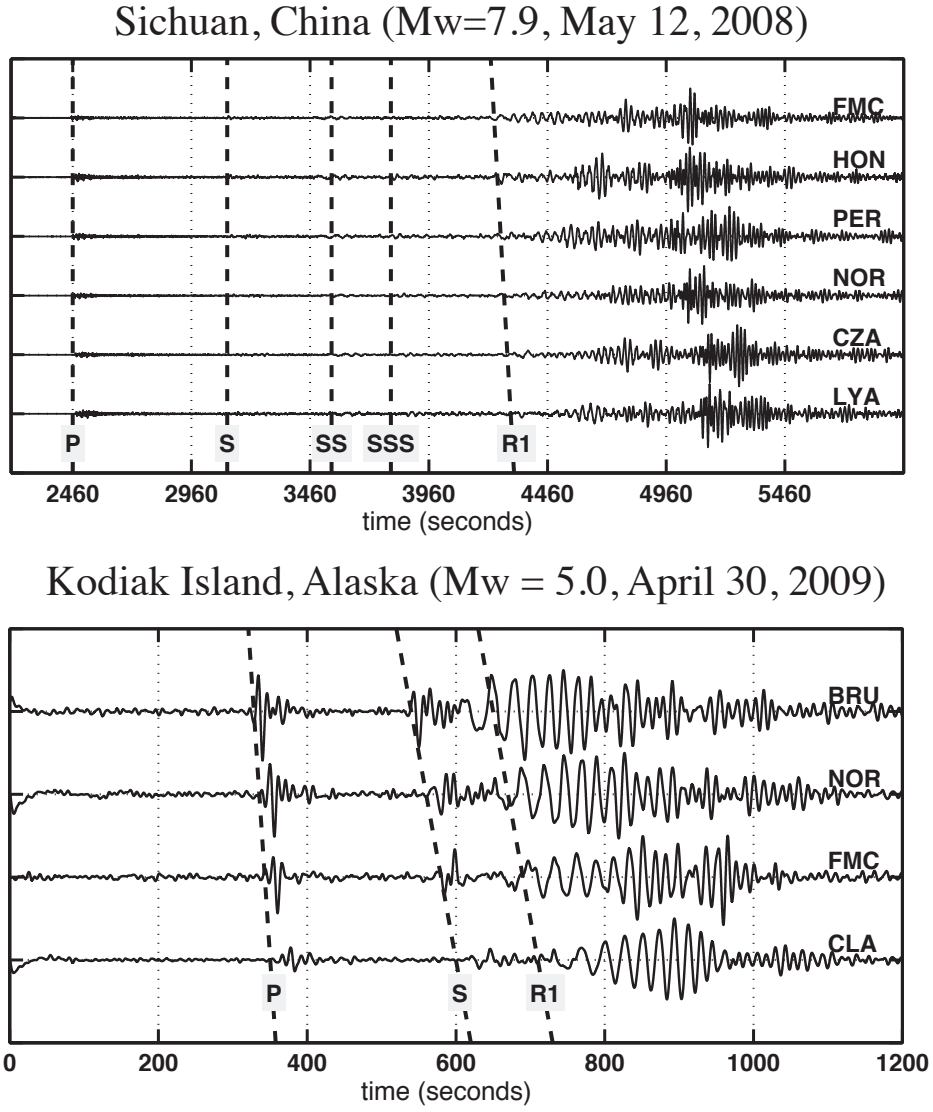


▲ **Figure 3.** Vertical-component waveforms at selected CRANE stations. The predicted arrival times and phase names are as indicated. The data from the Alaska event have been bandpass filtered to the frequency range of 0.03–0.06 Hz.

protect against water or animal-related damages, 2) reduce instrument noise associated with severe diurnal temperature changes, and 3) maintain the functionality of compact flash-cards (4–8 Gigabytes) during the harshest winter conditions. Despite our extensive efforts to optimize site selection and installation, one of the original sites (REC) had to be relocated after approximately eight months due to severe ground distortion in response to frost heaves.

Most of the CRANE stations have been operating continuously since early 2007, recording more than 500 $Mw > 5$ earthquakes over the past three-plus years. Figure 3 shows sample waveforms from a devastating $Mw$ 7.9 earthquake (Sichuan, May 2008) and a modest $Mw$ 5.0 earthquake in Alaska (April 2009). In both cases, body ($P$ and $S$) and surface wave arrivals are consistently identified on the vertical-component seismograms. Due to shallow vault depths, the quality of the horizontal component at most of the CRANE stations is adversely affected by noise associated with local weather conditions.

In addition to teleseismic earthquakes, the CRANE array has successfully recorded several smaller-magnitude ($Mw < 4.5$) events at regional (<10°) epicentral distances from Alberta, British Columbia, Washington, Oregon, and Montana. Figure 4 shows the unfiltered vertical-component waveforms from an $Mw$ 3.5 earthquake near Lethbridge, Alberta. Strong high-frequency (>1 Hz) signals are observed at the closest stations (CLA and LYA, <300 km) to the earthquake epicenter. The timing of the $P$-wave arrivals, which roughly correlates with epicentral distance, is highly sensitive to the crustal structures sampled by the ray paths. Severe amplitude falloffs at high frequencies reflect strong ground attenuation within the uppermost sedimentary layer of the WCSB.

The data analysis phase of the infrastructure project is currently underway. Ongoing efforts emphasize the investigation of seismic structure and microseismic sources in Alberta. We combine teleseismic body/surface waves with "noisy" (or, uneventful) parts of continuous seismic recordings to provide

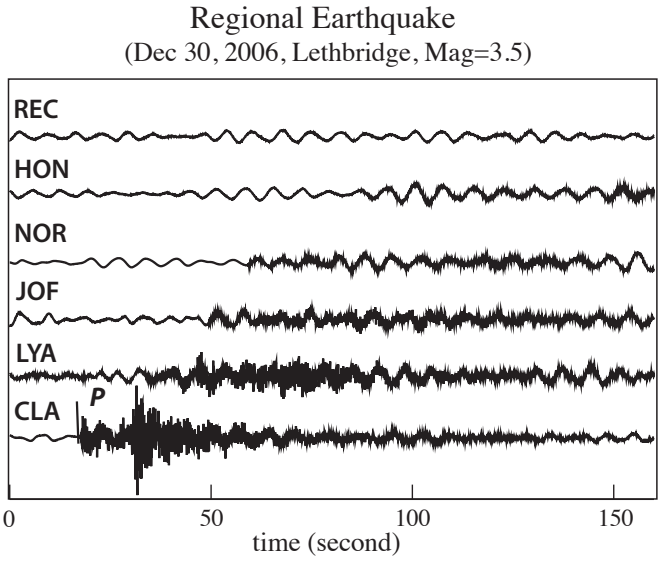


▲ **Figure 4.** Unfiltered waveforms from a regional earthquake (see Figure 1 for the geographical location of the earthquake). Significant high-frequency signals are observed at stations (*e.g.*, CLA, LYA) near the epicenter, though the signal appears to decay substantially at more distant stations (*e.g.*, REC) due to strong ground attenuation. Also visible on these records is a persistent ~8-sec microseismic signal.

detailed subsurface constraints. Considerable progress has been made in mapping regional seismic structure, local earthquakes, microseisms, and anisotropy. For brevity we only highlight preliminary results using receiver function, shear-wave splitting, and ambient seismic noise observations.

## PRELIMINARY RESULTS

### Tectonic Setup and Motivation

Tectonically, Alberta represents an important part of western Canada, a diverse geological framework consisting of Archean craton(s), Proterozoic orogens, and associated accretionary margins (known as "terranes"). The crust and mantle structure in the central and southern portion (Figure 5) underscores the Precambrian tectonic development of western Laurentia and more recent interactions between the North American craton and Cordilleran orogen (Hoffman 1988; Ross *et al.* 2000). Substantial thermal and tectonic overprinting has been proposed (Ross and Eaton 2002; Aulbach *et al.* 2004; Mahan and Williams 2005; Beaumount *et al.* 2010), possibly in connection with the Trans-Hudson orogen east of this region (see Figure 5) (Hoffman 1988; Bank *et al.* 1998; Zelt and Ellis 1999). The western edge of the sedimentary basin is demarcated by the Canadian Rockies, a part of the Western Cordillera likely formed in the late Cretaceous and early Tertiary during the Laramide orogeny (Livaccari *et al.* 1981; Maxson and Tickoff 1996; English and Johnson 2004; Cook *et al.* 2010; Liu *et al.* 2010). While regionally deep Moho interfaces have been observed and interpreted as the isostatic response to loading of the lithosphere by Mesozoic thrust sheets (*e.g.*, Price 1981; Cook 1995, 2002), the cause of the Laramide phase of mountain building and its effect on crust/lithosphere thickness remains uncertain (English and Johnson 2004; Liu *et al.* 2010)

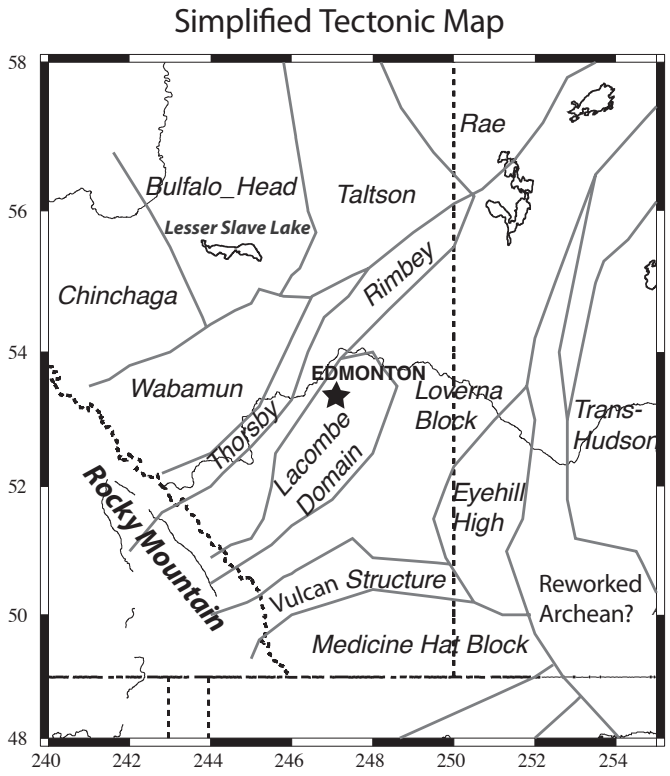


▲ **Figure 5.** A simplified tectonic map of the study area after Ross *et al.* (1991) and Shragge *et al.* (2002). Some of the domains could have undergone significant modifications and the boundaries between them remain debated.

Evidence from regional gravity, magnetic, and seismic surveys (see Ross 2000 and references therein; van der Lee and Frederiksen 2005; Marone and Romanowicz 2007; Courtier *et al.* 2010; Yuan and Romanowicz 2010) suggests the presence of major seismic velocity gradients and shear wave anisotropy beneath a broad spectrum of tectonic domains (*e.g.*, Buffalo Head, Wabamum, Thorsby, Lacombe, Eyehill, and Loverna; Hoffman 1988; Ross *et al.* 2000; Clowes *et al.* 2002) (see Figure 5). The age and origin of these domains and the extent of tectonic overprinting (*e.g.*, Ross and Eaton 2002) remains questionable. A key objective of our research is to reach a better understanding of the boundary and vertical extent of surface tectonics through the depths of crust/mantle interfaces, anisotropy, and wave speeds.

### Moho Imaging Using Receiver Functions

Among the various approaches we select *P*-to-*S* converted waves as a baseline constraint on deep-crustal and shallow-mantle stratigraphy. The use of converted waves, both *P*-to-*S* and *S*-to-*P*, as an imaging tool has an extensive history dating back to the mid-1970s (*e.g.*, Vinnik 1977; Langston 1979; Gurrola *et al.* 1994; Park and Levin, 2000;

Zhu and Kanamori 2000; Yang *et al.* 2006; see also Rondenay 2009 for a detailed review). In a nutshell, a body

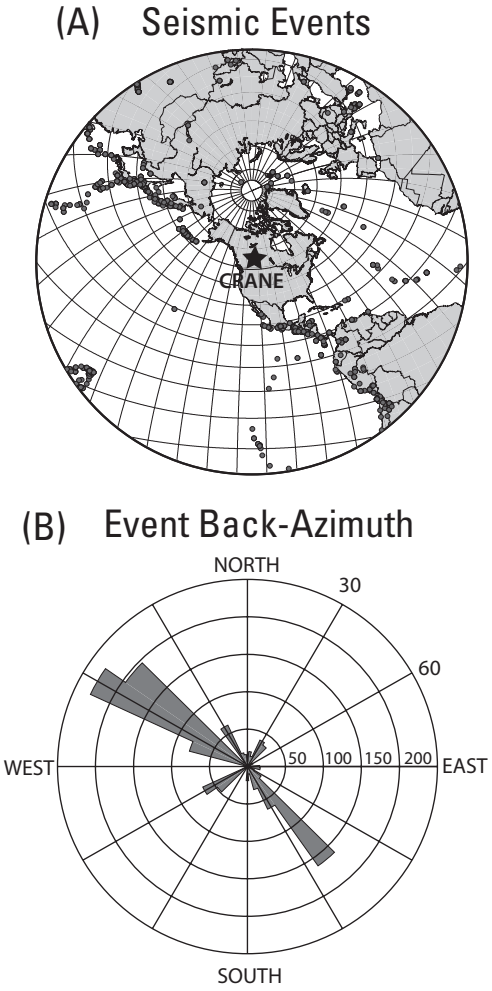


▲ **Figure 6.** A) More than 500 $Mw > 5$ earthquakes (1,204 source-station pairs) used in our receiver-function analysis. B) A rose diagram showing the distribution of station back-azimuths to the earthquakes. The non-uniform path coverage shows a dominant NW-SE orientation.

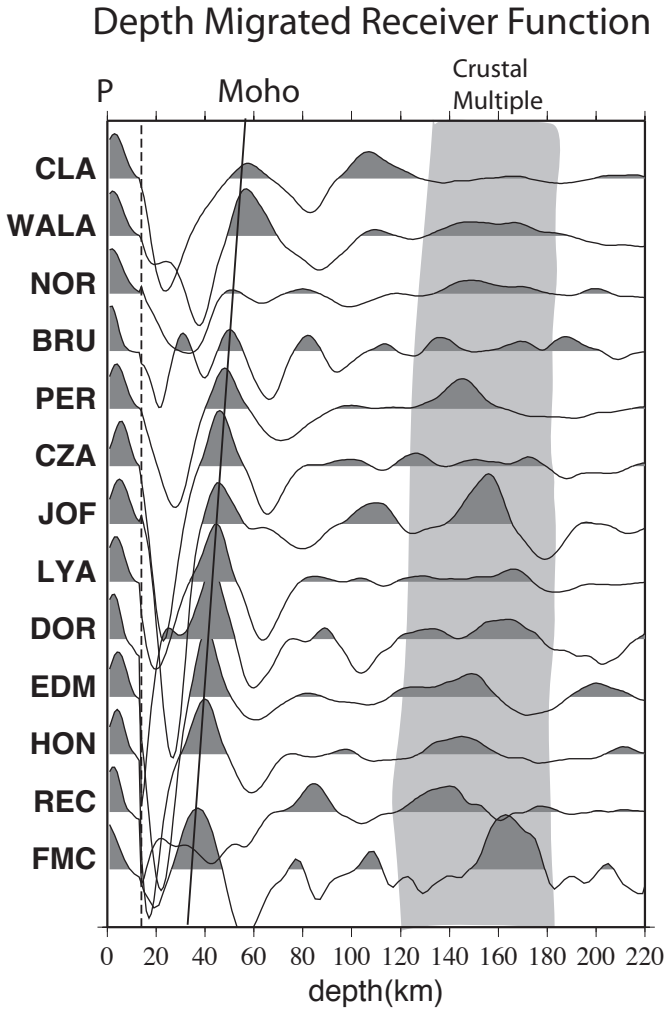


▲ **Figure 7.** Stacked radial-component receiver functions from the CRANE and CNSN stations (see Figure 1). Clearly visible are strong crustal conversions, multiples (which can interfere with reflectors in the depth range of 140–180 km), and potential reflectors from 80 to 120 km. The thickness of the sedimentary cover can also be estimated from the delay of radial *P* arrivals relative to the origin depth. The Moho interface shows substantial lateral variations in reflection amplitude and depth.

wave encountering a discontinuity in material properties is partitioned into transmitted and reflected waves. The arrival time difference between the direct *P* wave and a subsequent conversion or reverberation is a sensitive indicator of the seismic velocity structure between the interface and receiver.

We construct a waveform database with 500+ $Mw > 5$ earthquakes recorded between 2007 and 2009 (Figure 6A). All earthquake-station pairs are restricted to the epicentral distance range of 30°–90° and the distribution of source-receiver paths shows a dominant NW-SE orientation (Figure 6B). Displacement seismograms from each event are filtered between corner frequencies of 0.04–1.0 Hz, a range that includes signals from both crust and mantle interfaces. At the final stage of data preparation, the two horizontal (E-W, N-S) components are rotated to radial and transverse orientations based on station back-azimuths. We then compute radial receiver functions for all stations through a water-level deconvolution approach (Ammon *et al.* 1990; Ammon 1991). For the preliminary analysis we adopt a water level of 0.02, which is determined through trial and error based on the noise level of a typical *Mw* 5.5 earthquake record. A Gaussian filter with a pulse width of 1.5 is subsequently applied to further suppress high-frequency noise.

Figure 7 shows the receiver functions for the available CNSN and CRANE stations after stacking over all azimuths. We convert these time-domain receiver functions to depth based on PREM (Dziewonski and Anderson 1981), which provides a first-order approximation for the depths of crust and mantle converters in the absence of more accepted regional *P* or *S* velocity models. If one assumes a travel time uncertainty of 1 sec and an epicentral distance of 60°, a net velocity perturbation of 2 km/sec (1 km/sec increase in mantle *P* velocity and 1 km/sec decrease in lower-crustal *S* velocity relative to PREM) will displace the Moho interface by ~2.6 km using the pertur-

bation theory introduced by Dziewonski and Gilbert (1976). With the exception of REC, which has a sizeable transverse-component signal, conversions from the crustal interface (for short, *Pms*, *m* for Moho) are clearly detected at depths ranging from 35 km beneath the northern part of the array (FMC) to 58 km beneath the southernmost station (WALA). The amplitude of *Pms* generally decreases toward the Rocky Mountain foreland, where a dipping Moho interface (Cassidy 1992) and/or anisotropy with a non-horizontal axis of symmetry (Levin and Park 1997) could be important. Significant timing (near 0 sec) and pulse width variations of the *P* phase on the radial receiver functions (see Figure 7) indicate slower, more complex radial-component signal relative to the vertical. Similar observations have generally been attributed to low-velocity sedimentary layers beneath seismic receivers (Cassidy 1992; Sheehan *et al.* 1995; Zelt and Ellis 1999). Depending on the thickness of this sedimentary layer, *Pms* at the base of this low-velocity layer could interfere with the direct *P* phase and cause ~1-sec delay on radial receiver functions (Sheehan *et al.* 1995; Mangino and Priestley 1998). Our preliminary results are consistent with the general outline of the sedimentary basin: for example, *Pms* observations in mountainous regions (*e.g.*, BRU, NOR, WALA) generally precede those in the heart of the southern WCSB (*e.g.*, EDM, JOF, HON, CZA) (see Figure 7). The maximum delay time (0.8 sec) of radial-component *P* phase is observed at station CZA, which translates to a sediment thickness of ~6 km based on PREM (Dziewonski and Anderson 1981) velocities.

The depth variation of the Moho interface from the CRANE stations improves the lateral resolution of existing regional models. A comparison with CRUST2.0 (Bassin *et al.* 2000; Figure 8), a 2° × 2° global model, shows remarkable consistency despite apparent resolution differences. For instance, the crust is nearly ~50 km thick underneath the Rockies north of 52° latitude, as suggested by BRU and NOR. The Moho depths beneath central Alberta range from 37 to 41 km, which are within 2 km of the values reported by CRUST2.0 and regional refraction/reflection surveys (Bouzidi *et al.* 2002).

Semi-linear cross-sections (see Figure 8 for orientations) show coherent trends in Moho depths (Figure 9). The crust thickens from north to south along path 1 and from west to east at low latitudes along path 2. The deepest crustal root (~58 km, WALA) is identified near the southern tip of the Canadian Rockies, which is consistent with regional estimates using exploration (SARAX; Clowes *et al.* 2002) and USArray (Levander and Miller 2010) data; values from all three studies are ~10 km thicker than that of CRUST2.0 (40–45 km, not plotted). An anomalously thick and seismically fast crust beneath southernmost Alberta has been attributed to 1) Proterozoic underplating of a fast, lower crustal layer (Clowes *et al.* 2002), and 2) subduction of the Shasky and Hess ocean plateaus during the Laramide phase of the mountain building (Livaccari *et al.* 1981; Liu *et al.* 2010). Mafic igneous rocks with relatively high density and seismic velocity (Lemieux *et al.* 2000; Mueller *et al.* 2001; Clowes *et al.* 2002), stishovite-structured silica originated by the post-stishovite phase transition within the subducted mid-ocean-ridge basalts (Carpenter *et al.* 2000), and eclogization of the mafic lower crust (Hynes and Snyder 1995; Fischer 2002) may further contribute to the enhanced lower-crustal seismic velocities in the latter hypothesis. On the other hand, consistently thick crust beneath the mountain belt appears to favor a mechanism that is inherent to the formation and evolution of the northern Rockies.

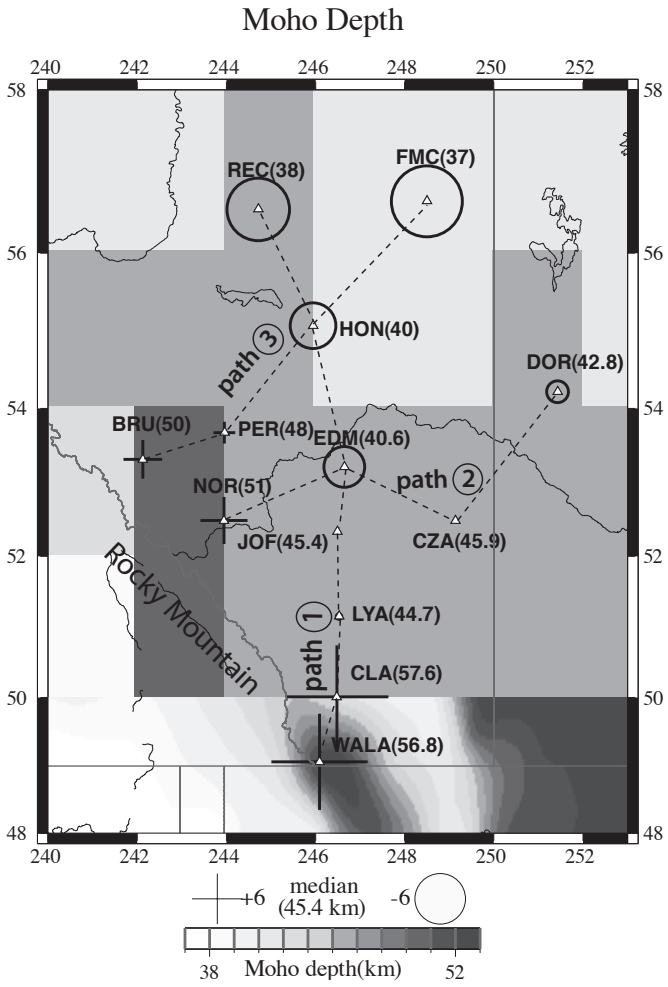


▲ **Figure 8.** Map of the Moho depth from our receiver function analysis. The low-resolution map above 50° latitude shows CRUST2.0 (Bassin *et al.* 2000) model values. The numerical value at each station location indicates the estimated crustal thickness in kilometers. The high-resolution map south of the 50° latitude shows the reported values from Levander and Miller (2010) based on USArray data. The crust beneath the Canadian Rockies (50–57 km) is considerably thicker than that beneath the adjacent plains (37–45 km). The dashed lines denote three semi-linear cross-sections through the study region.

Moho depth variations from receiver function analysis could aid our efforts in mapping the crustal domains within the Alberta Basin. On average, the crust is ~5 km thicker under the proposed southern edge of the Loverna block (~51° latitude, near JOF, LYA, and CZA) than in the Lacombe domain (Clowes *et al.* 2002; Cook *et al.* 2010). The crustal root continues to shallow under the juxtaposed Precambrian domains

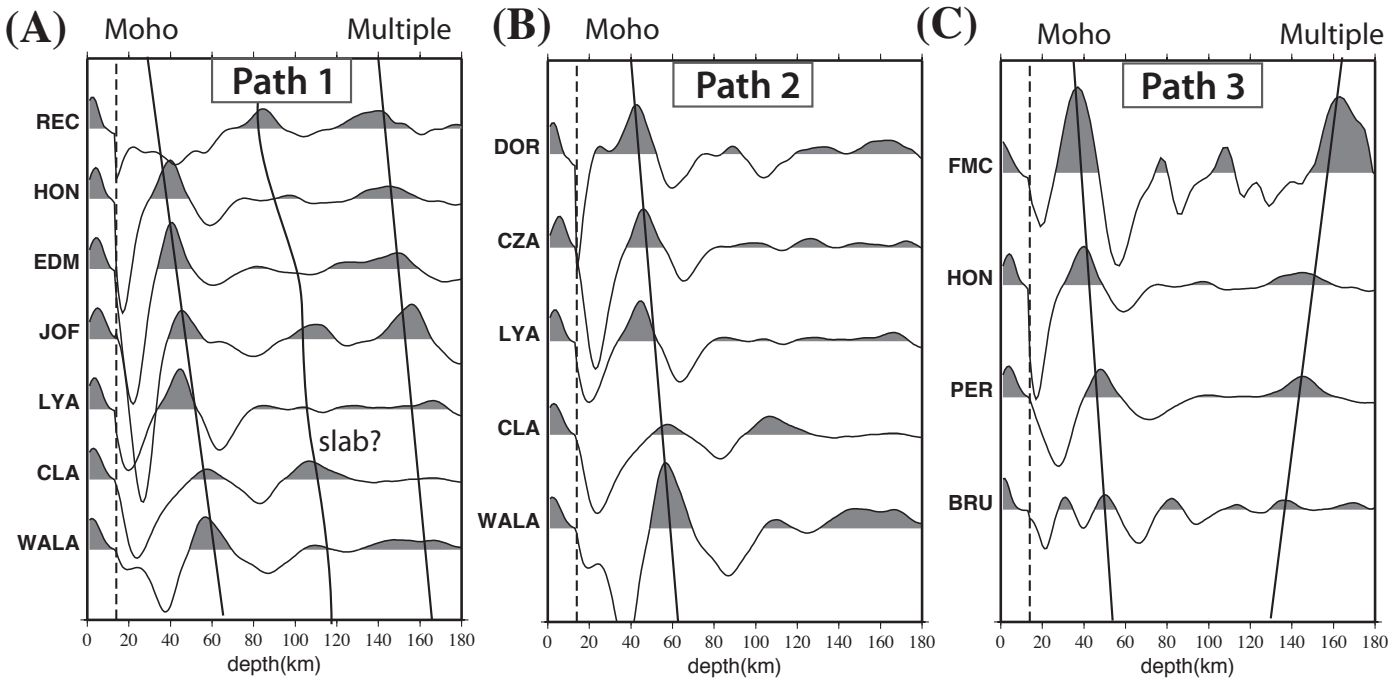


▲ **Figure 9.** Receiver functions from a N-S and two E-W cross-sections (see Figure 8). The crust gradually thickens toward the U.S.-Canadian border. Also visible is a thick and weakly reflecting crustal layer beneath the Rockies. The N-S section contains an unexplained phase arriving at the conversion depths of 90–130 km. This converted signal could be associated with past subducted oceanic lithosphere.

consisting of Rimbey, Taltson, and Buffalo Head (near FMC and REC). The thickness differences between these domains (2–5 km) fall below the statistical measurement uncertainties (1–2 km) and are highly consistent with reported values from earlier active source experiments (see Bouzidi *et al.* 2002; Clowes *et al.* 2002; Cook 2002).

### Seismic Anisotropy

As is true of crustal thickness variations, surface tectonics could have far reaching implications for the understanding of seismic anisotropy. Due to an extensive strain history that includes episodes of faulting, magmatism, accretion, and subduction (Hoffman 1988; Ross *et al.* 2000), permanent deformation would be expected below the WCSB at mantle depths and a direct consequence is seismic anisotropy, where olivine's crystollographic fast axis is preferentially aligned with the direction of maximum shear or least compression.

In this phase of the array analysis we select multiple magnitude $Mw > 6.5$ earthquakes recorded at every CRANE station and examine *SKS* splitting (Bowman and Ando 1987; Silver and Chan 1991; Menke and Levin 2003; Gu *et al.* 2009), a phenomenon often interpreted as the consequence of anisotropy similar to optical birefringence of minerals under polarized light (see review by Long and Silver 2009). The splitting parameters, which consist of delay time (between the fast and slow shear waves) and fast polarization azimuth, directly reflect the strength and direction of anisotropy. In this analysis each measurement is made based on the cross-convolution method for multiple earthquakes (Menke and Levin 2003) and then independently confirmed by the rotation correction method (Bowman and Ando 1987), minimum energy method (Silver and Chan 1991), and eigenvalue method (Silver and Chan 1991). The majority of the stations are constrained by more than 10 earthquakes, with the glaring exception of HYLO where only one earthquake is available due to a late deployment schedule. Both single- and two-layer anisotropy are considered for each station based on waveform correlations. Finally, the delay times and azimuth uncertainties are determined by a bootstrap resampling algorithm (Efron and Tibshirani 1991) using randomly selected subsets of earthquakes.

Our preliminary analysis of the CRANE array data shows clear evidence of shear wave splitting. The particle motions for *SKS* phases after correcting for anisotropy are approximately linear, as would be expected for an isotropic mantle (Figure 10). Splitting parameters vary systematically across the CRANE array (Figure 11): the majority of the measurements along the Rocky Mountain foothills (*e.g.*, CLA, LYA, NOR, BRU) are oriented along a NE-SW orientation and show consistently large (~1.5–1.9 sec) time delays; in comparison, substantially lower splitting time delays are observed beneath eastern-central Alberta where the fast axes appear tangential to a N-S trending ellipse centered at 200–300 km northeast of Edmonton.

The splitting parameters in the vicinity of the Canadian Rockies suggest strong "order" in mantle mineralogy (Long and Silver 2009). The NE-SW trending fast direction is consistent with previously reported values utilizing Lithoprobe data (Shragge *et al.* 2002) and the direction of maximum horizontal stress—a proxy for the "fossil" strain field within the lithosphere in response to the past episodes of NW-SE plate convergence and subduction of Farallon and Kula plates (*e.g.*,

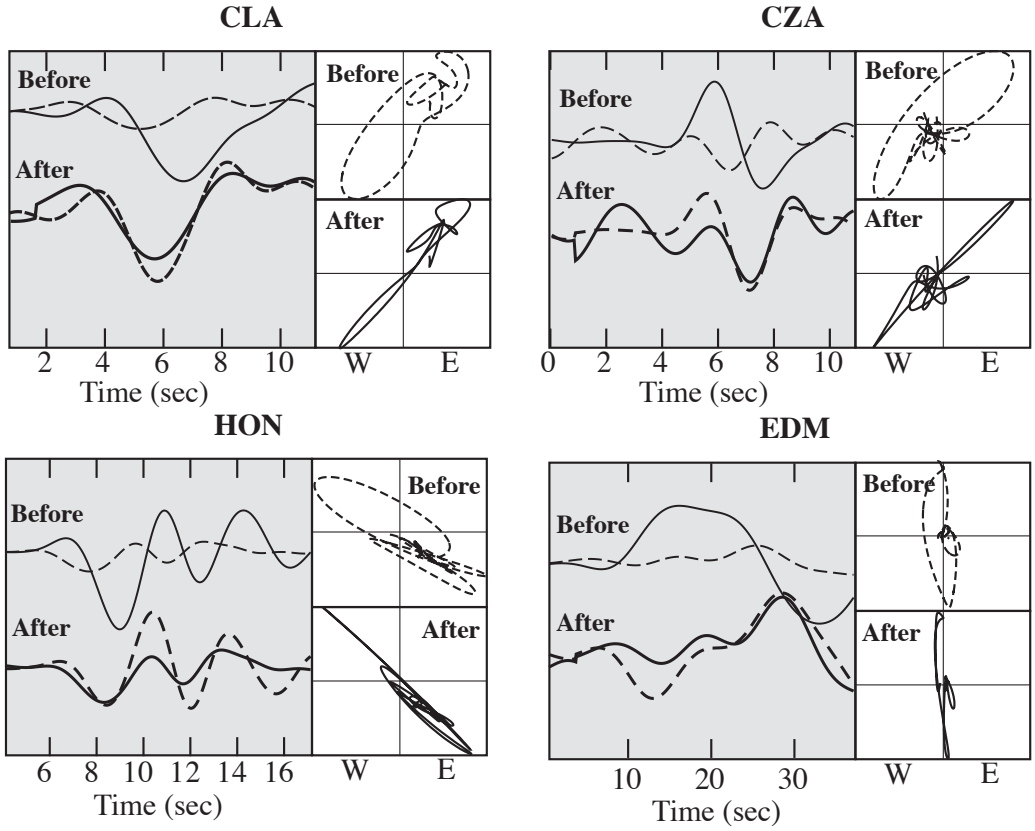


▲ **Figure 10.** Sample cross-convolution functions and particle motions from our shear-wave splitting analysis. For the majority of the CRANE/CNSN stations, the inverted splitting parameters not only improve the agreement between the horizontal-component cross-convolution functions (left panel; see Menke and Levin 2003) but also increase the linearity of the particle motion (right panel).

Helmstaedt and Schulze 1989; Ross *et al.* 2000). The combination of pre-existing fabric within the mantle lithosphere and the present-day absolute plate-motion, which is, coincidentally, NE-SW, offers an attractive explanation for the large *SKS* delays and 3–6% azimuthal anisotropy in this region. Without further data constraint it is, however, difficult to resolve the full history of mantle deformation or the number of anisotropic layers (*e.g.*, Shragge *et al.* 2002; Marone and Romanowicz 2007).

The origin of the complex shear-wave splitting pattern beneath eastern-central Alberta remains unclear. It could potentially be linked to the adjacent Buffalo Head terrane, a region that has attracted national attention in recent years due to the discovery of precious minerals. The vicinity of the anisotropic anomaly exhibits enhanced heat-flow (Blackwell and Richards 2004) and below-average seismic velocity (van der Lee and Frederiksen 2005) and Bouguer gravity values. The presence of a divot (Fouch *et al.* 2000) or an abandoned plume conduit (Bank *et al.* 1998) on the continental root offers a viable explanation. On a local scale, geometrical imperfection associated with past plate interactions could trap hot asthenospheric material and disrupt the mantle flow around it. Within a larger tectonic framework, the anomalous shear-wave splitting observations in eastern-central Alberta could signal a hidden tectonic boundary between stable continents (east/northeast) and accreted terranes (west). For instance, streamlined mantle flow around the edges of moving continental "keels" (*e.g.*, Gaherty and Jordan 1995; Ben Ismail and Mainprice 1998; Bokelmann and Silver 2002) can induce strong N-S oriented horizontal strain. In other words, shear deformation at the base of the lithosphere (~200 km) and disrupted flow at shallower depths could both be present, producing complex, multilayered anisotropy in this region. Furthermore, due to the substantial topographical relief on the base of the lithosphere (Hyndman *et al.* 2005), both radial and azimuthal anisotropy would be expected in this transitional region.

The aforementioned shear wave splitting results show only one integral component of our infrastructure project. Interpretations aside, the data from CRANE present a window of opportunity to visualize the present state and geometry of the continental lithosphere. Expected outcomes of the ongoing research efforts may ultimately contribute to the discussion of the mechanism(s) by which lithosphere evolves from thin convergent margins to thick, depleted continental roots.

### Ambient Noise Group Velocities

Accurate interpretations of reflectivity and anisotropy (discussed in the two previous sections) can greatly benefit from improved knowledge of the seismic velocities at crust and mantle depths. For this reason, our ongoing research effort aims to provide accurate, high-resolution $P$ and $S$ velocity models in the study region using both earthquake recordings and ambi-

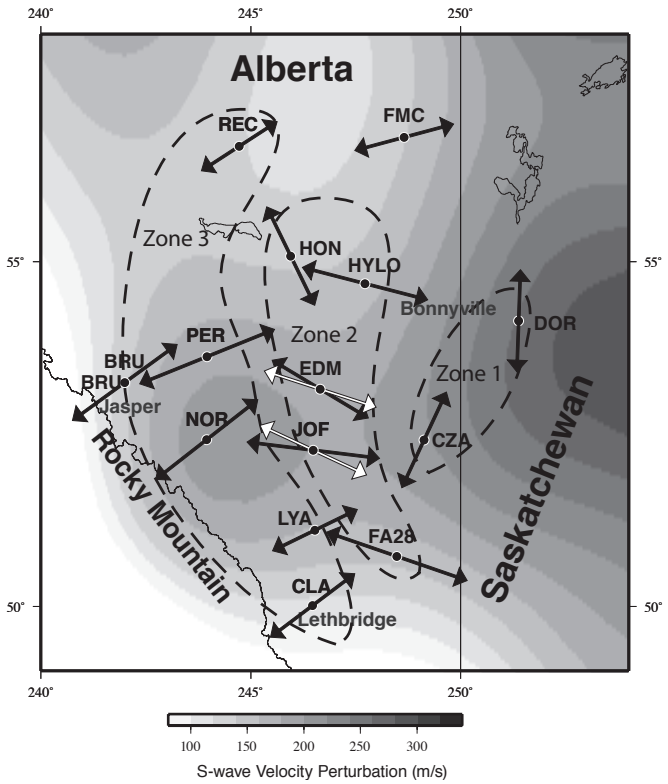


▲ **Figure 11.** *SKS* splitting vectors superimposed on an updated shear velocity map of van der Lee and Frederiksen (2005). Double arrows at a given station indicate potential two-layer anisotropy. The splitting directions change rapidly with distance from the Rockies. Three distinct zones are present: Zone 3 suggests strong anisotropy associated with past and present-day plate motions, whereas Zone 1 and Zone 2 are likely caused by disrupted mantle flow around a migrating continental keel.

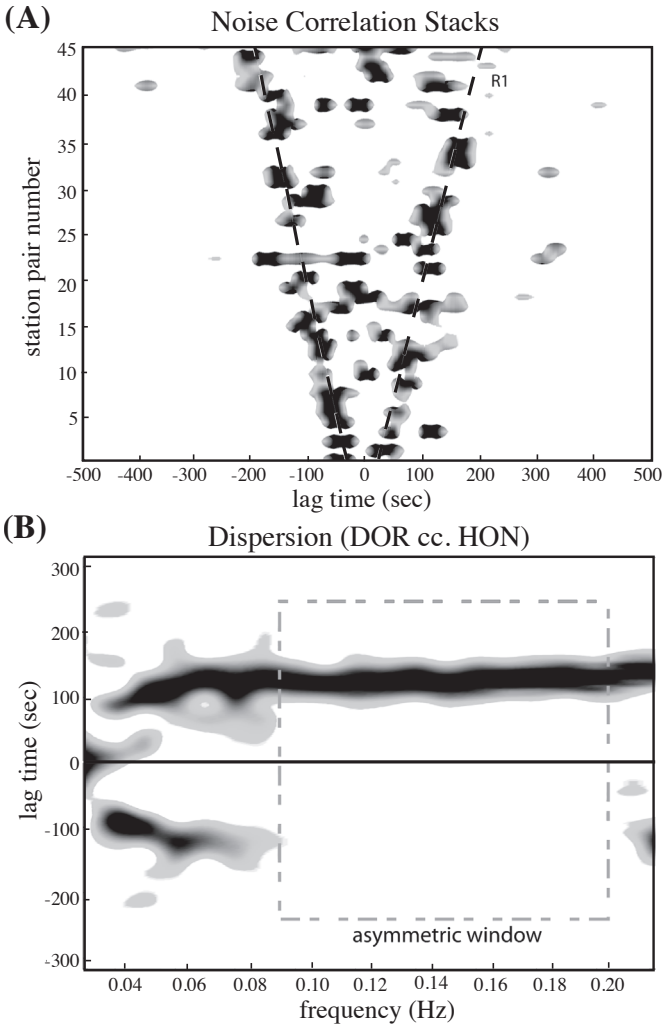


▲ **Figure 12.** A) Vertical-component cross-correlation functions of seismic noise, computed from a full year of CRANE station recordings. The scale on the y-axis is nonlinear and only approximates the true distance between any two stations. A bandpass filter (0.03–0.06 Hz) has been applied to the original cross-correlation functions. B) Dispersion curves computed from multitapered correlation functions. The decreased lag times at low frequencies are caused by higher wave speeds (relative to the Earth's surface) at lower-crustal/shallow-mantle depths. The apparent asymmetry in the frequency range of 0.08–0.2 Hz suggests the presence of a potential non-ambient noise source.

ent noise correlation functions (Longuet-Higgins 1950; see review by Weaver 2005). Figure 12 shows inter-station noise correlation stacks computed from continuous vertical-component records between 2007 and 2009. The distance-time moveout and sample dispersion curves highlight ambient Rayleigh wave arrivals between the CRANE stations. The lag times of the correlation peaks (see Figure 12A) offer reliable constraints on regional shear/Rayleigh wave speeds (Shapiro *et al.* 2005; Yang *et al.* 2006; Bensen *et al.* 2007) and anisotropy (*e.g.*, Yao *et al.* 2006) down to ~100 km depth. While persistent noise sources may be present due to correlation asymmetry (Gu *et al.* 2007; Yang and Ritzwoller 2008; Brzak *et al.* 2009) (Figure 12B), signals from the majority of the station pairs are accurate enough for a tomographic analysis under the "ambient noise" assumption (see Weaver 2005).

We determine group velocities of Rayleigh waves via inversions of the arrival times of noise-correlation peaks (*e.g.*, Shapiro *et al.* 2005; Bensen *et al.* 2007; Yang *et al.* 2011). The study region is divided into uniform cells (area = ~100 km$^2$) (Kennet *et al.* 1988) and the inversion algorithm is based on the fast matching method (Rawlinson and Sambridge 2005). Regularization factors pertaining to the norm and gradient of velocities are determined independently based on tradeoff curves. The inverted group velocities significantly reduce the variance of correlation-based travel time residuals at two distinct frequency ranges (Figure 13). The skew caused by the biases of the starting model is also minimized and the distributions of the residuals are approximately Gaussian after the inversion. These improvements are particularly evident at longer periods (see Figure 13B) where noise correlation peaks are more reliably measured.

Figure 14 shows the inverted group velocity maps for frequency ranges of 0.10–0.16 Hz and 0.06–0.10 Hz. The former

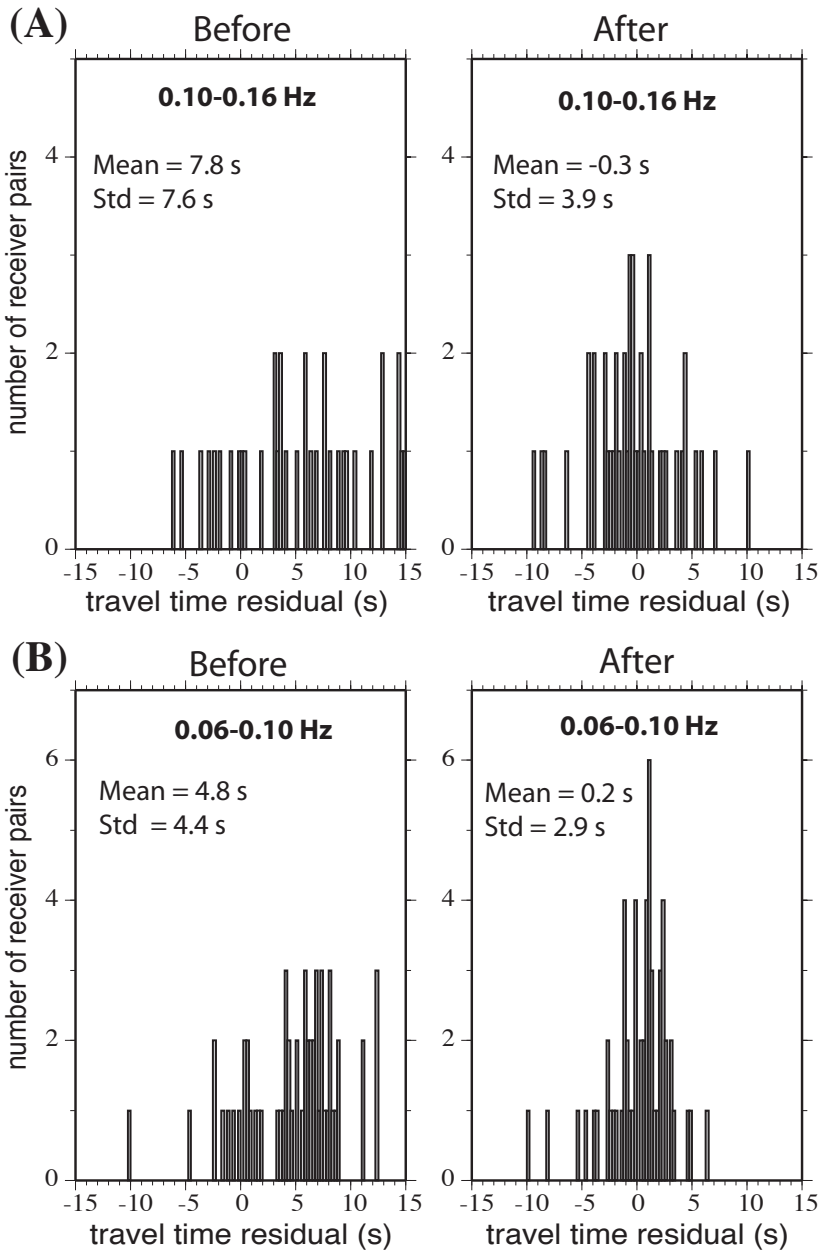


▲ **Figure 13.** Noise correlation–based travel-time residuals before and after least-squares group velocity inversions for frequency ranges of (A) 0.10–0.16 Hz, and (B) 0.06–0.10 Hz. The residuals are computed by removing travel-time predictions of a constant starting (left panels) and best-fit (right panels) models. The residual distributions are approximately Gaussian after the inversions.

pass-band (Figure 14A) is mainly sensitive to the basement structure beneath the study region, whereas frequencies lower than 0.1 Hz offer greater constraints on the rock properties below mid-crust. Both pass-bands show peak-to-peak group velocity variations in excess of 0.8 km/s, indicating strong lateral heterogeneities throughout the crust. The upper crust beneath the Alberta Basin, particularly the region enclosed by stations CZA, JOF, CLA, WALA, A17, and A18, is consistently slower than the foothills of the northern Rockies (see Figure 14A). The overall correlation between velocity and basement domains is lower than expected, however, suggesting significant tectonic overprinting since the formation of these domains (*e.g.*, Ross and Eaton 2002; Beaumount *et al.* 2010). Low seismic velocities are further identified beneath the Wabamum domain, the Taltson magmatic belt, and the northern Rockies southwest of the Thorsby domain (see Figure 5 and Hoffman 1988; Ross *et al.* 1991). Among them, the anomaly beneath station SLEB (labeled "1" in Figure 14) extends well below mid-crust, as suggested both by Figure 14B and by frequencies lower than 0.03 Hz (not shown). Geographically, this structure resides directly west of the proposed Cordilleran deformation front by Mercier *et al.* (2009) and supports a sharp transition from fast (east of the boundary) to slow (west of the boundary) lower-crust and upper-mantle wave speeds. Unfortunately, a direct comparison of velocities is not possible due to a visible gap in data coverage in Mercier *et al.* (2009). Farther east, our model shows consis-

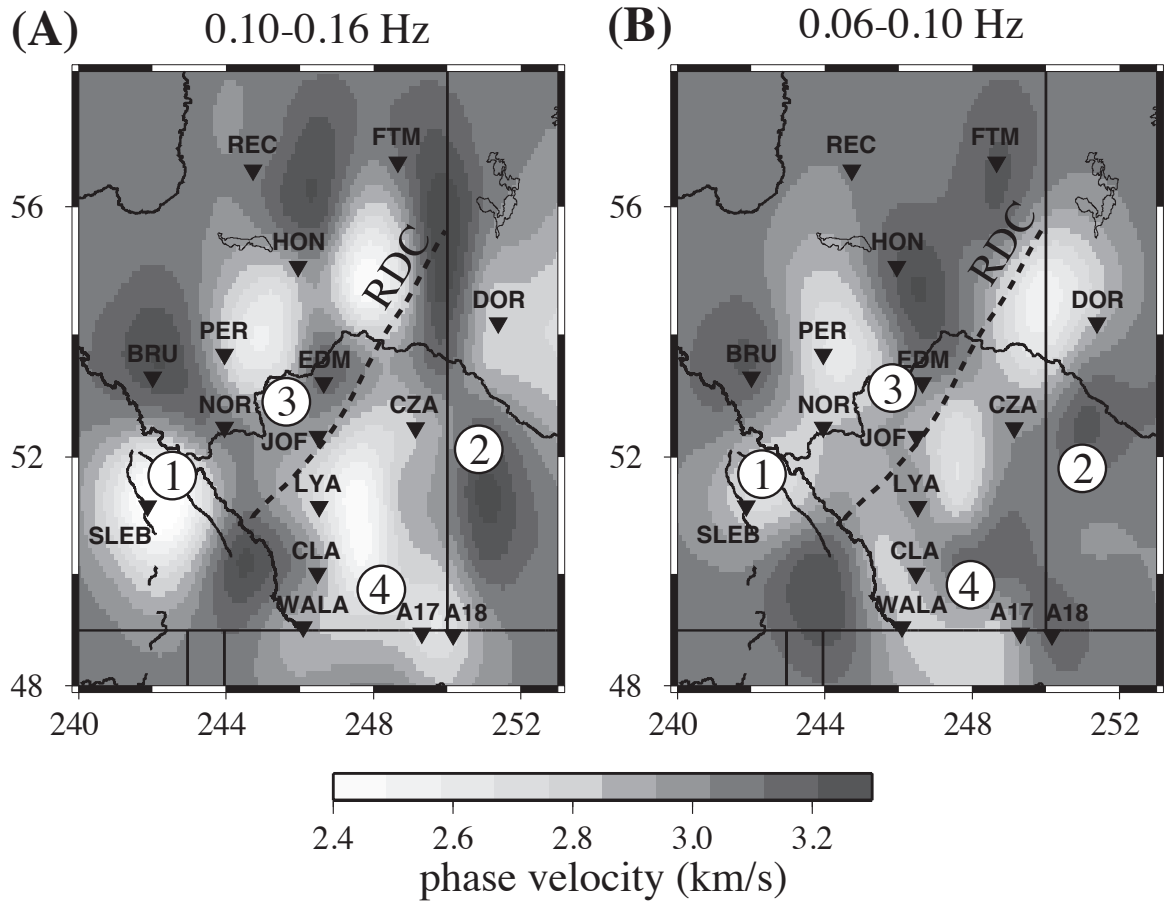


▲ **Figure 14.** Inverted group velocities using the lag times of noise correlation peaks. The correlation functions are filtered between corner frequencies of (A) 0.10 Hz and 0.16 Hz and (B) 0.06 Hz and 0.10 Hz. Signals in these two frequency ranges are sensitive to the upper-middle crust (panel A) and lower crust/upper mantle (panel B), respectively. The dashed line shows the Red Deer conductor (RDC) (Boerner *et al.*, 1995; Boerner *et al.* 2002). The peak-to-peak variation in group velocity is as large as ~0.8 km/sec. See text for detailed explanations of the numbered regions.

tently high shear velocities beneath the southeastern provincial boundary between Alberta and Saskatchewan (labeled "2" on Figure 14). The crust and lithospheric mantle beneath this region could be dominated by rocks of Archean (or reworked Archean) age (*e.g.*, Ross *et al.* 1991; Shragge *et al.* 2002), as suggested by sharply increased mantle velocities in recent models of high-resolution seismic tomography (see Figure 11; van der Lee and Frederiksen 2005; Nettles and Dziewonski 2008).

Interpretations of some of the heterogeneous structures from this preliminary study (see Figure 14, labeled "3" and "4") could be more controversial. For instance, streaking high velocities are observed near stations EDM and JOF and extend southwestward toward the foothills of the Rockies. This anomaly roughly coincides with a vertically continuous, high-velocity structure in Shragge *et al.* (2002), and its proximity to the Red Deer conductor (RDC) raises the possibility of a regionally positive (rather than often-assumed negative) correlation between seismic velocity and electrical conductivity (see Shragge *et al.* 2002 for detailed discussions). The width of the RDC is critical since, at different frequencies, both increased shallow-crustal (see Figure 14A, slightly north of the dashed line) and decreased lower-crustal (see Figure 14B, south of the dashed line) wave speeds could be associated with this conductive anomaly.

Structure surrounding the Medicine Hat Block (MHB) provides another example of existing uncertainties about the history of the WCSB. Initially, this region was associated with the Hearn Province (Ross *et al.* 1991; Eaton *et al.* 1999) north of the Great Falls tectonic zone (Hoffman 1988), though more recent observations have favored a deformation history more consistent with that of an autonomous craton segment (*e.g.*, Eaton *et al.* 2000; Gorman *et al.* 2002; Clowes *et al.* 2002). Intrusions of mafic sills under the Precambrian basement (Lemieux *et al.* 2000; Mueller *et al.* 2001; Welford and Clowes 2004) and the emplacement of a high-velocity lower crust via Proterozoic underplating (Gorman *et al.* 2002; Clowes *et al.* 2002) have been proposed for this region. These exploration-based inferences are, to a significant extent, at odds with models based on global (*e.g.*, van der Lee and Frederiksen 2005; Nettles and Dziewonski 2008) and regional (Shragge *et al.* 2002) broadband seismic data. While an argument could be made against global tomography on the basis of limited spatial resolution, the lack of more distinctive signatures surrounding the MHB in the regional body-wave model is indeed

enigmatic. Our regional noise-correlation tomography shows increased surface wave group velocities below mid-crust, especially east of 114° W at low frequencies (see structure labeled "4" in Figure 14) near Medicine Hat and the adjacent Vulcan regions. This anomaly appears to persist down to ~50 km (and possibly deeper) according to noise-correlation peaks at frequencies below 0.03 Hz. The segmented appearance and limited strength of this high-velocity "tongue" remain problematic, though its presence would provide marginal support to the hypothesis of Proterozoic underplating where decreased density and increased iron content are not explicitly required in the lower crust and upper mantle (see Shragge *et al.* 2002).

As mentioned earlier, the tomographic imaging of regional *P* and *S* velocities remains a work in progress. Hence, the results shown in this section are only preliminary in nature and require more rigorous analyses of data accuracy and resolution. In time, the rich datasets offered by CRANE and existing regional broadband stations should vastly improve the regional structural constraints on the southern WCSB.

## CONCLUSIONS

The establishment of the CRANE array opens a new chapter in regional seismicity monitoring and crust/mantle imaging in Alberta and nearby regions. The array deployment schedule and the geometry complement the USArray project, the leading international initiative with dense seismic and magnetotelluric arrays presently deployed southeast of Alberta. The high-quality data records from CRANE have shown significant promise in both seismic source and structure analyses, the latter being evidenced by the preliminary results presented in this article. This project will foster further in-province and cross-border multidisciplinary collaborations. By integrating a wide range of data constraints and methodologies, the nature of the seismic anomalies presented in this study, as well as other fundamental properties of the southwestern Canadian subsurface, will become clearer in the near future. Additional information pertaining to the array project can be found in the recent *Edmonton Journal* article "Alberta's seismic pulse gets a reading" (June 10, 2009) and *Rocky Mountain House Mountaineer* article "Nordegg Earthquake research aids Alberta scientists" (June 23, 2009). Continuous data from CRANE, presently managed by the Incorporated Research Institutions for Seismology (IRIS) Data Management centers, are open to the general public.

## ACKNOWLEDGMENTS

We sincerely thank Dinu Pana, David Snyder, Virginia Stern, and Corey Froese for their scientific input and support of the instrument project. We also thank all of the hosts of our seismic stations. Their passion for fundamental scientific research is exemplary. This instrument project also benefited from two constructive reviews, as well as from technical assistance from the CNSN and IRIS Data Management Center. This project is jointly funded by CFI, Alberta Innovates, Alberta Geological Survey, National Science and Engineering Council (NSERC), and the University of Alberta.

## REFERENCES

Ammon, C. J. (1991). The isolation of receiver effects from teleseismic P waveforms. *Bulletin of Seismological Society of America* **81**, 2,504–2,510.

Ammon, C. J., G. E. Randall, and G. Zandt (1990). On the non-uniqueness of receiver function inversions. *Journal of Geophysical Research* **95**, 15,303–15,318.

Aulbach, S., W. L. Griffin, S. Y. O'Reilly, and T. E. McCandless (2004). Genesis and evolution of the lithospheric mantle beneath the Buffalo Head terrane, Alberta (Canada). *Lithos* 77, 413–451.

Bank, C.-G., M. G. Bostock, Z. Hajnal, and J. C. VanDecar (1998). Lithospheric mantle structure beneath the Trans-Hudson orogen and the origin of diamondiferous kimberlites. *Journal of Geophysical Research* **103**, 10,103–10,114.

Bassin, C., G. Laske, and G. Masters (2000). Current limits of resolution for surface wave tomography in North America. *Eos, Transactions, American Geophysical Union* **81**, F897.

Beaumont, C., R. Jamieson, and M. Nguyen (2010). Models of large, hot orogens containing a collage of reworked and accreted terranes. *Canadian Journal of Earth Sciences* **47**, 485–515.

Ben Ismail, W., and D. Mainprice (1998). An olivine fabric database: An overview of upper mantle fabrics and seismic anisotropy. *Tectonophysics* **296**, 145–157.

Bensen, G. D., M. H. Ritzwoller, M. P. Barmin, A. L. Levshin, F. Lin, M. P. Moschetti, N. M. Shapiro, and Y. Yang (2007). Processing seismic ambient noise data to obtain reliable broad-band surface wave dispersion measurements. *Geophysical Journal International* **169**, 1,239–1,260; doi:10.1111/j.1365-246X.2007.03374.x.

Bird, P. (1998). Kinematic history of the Laramide orogeny in latitudes 35-49 N, western United States. *Tectonics* **17**, 780–801.

Blackwell, D. D., and M. Richards (2004). *Geothermal Map of North America*. American Association of Petroleum Geologists (AAPG), 1 sheet, scale 1:6,500,000.

Boerner, D. E., R. D. Kurtz, J. A. Craven, G. M. Ross, and F. W. Jones (2002). A synthesis of electromagnetic studies in the Lithoprobe Alberta Basement Transect: Constraints on Paleoproterozoic indentation tectonics. *Canadian Journal of Earth Sciences* **37**, 1,509–1,534.

Bokelmann, G., and P. G. Silver (2002). Shear stress at the base of shield lithosphere. *Geophysical Research Letters* **29**; doi:10.1029/2002GL015925.

Bouzidi, Y., D. R. Schmitt, R. A. Burwash, and E. R. Kanasewich (2002). Depth migration of deep seismic reflection profiles: Crustal thickness variations in Alberta. *Canadian Journal of Earth Sciences* **39**, 331–350.

Bowman, J. R., and M. Ando (1987). Shear wave splitting in the upper-mantle wedge above the Tonga subduction zone. *Geophysical Journal of the Royal Astronomical Society* **88**, 25–41.

Brzak, K., Y. J. Gu, A. Okeler, M. Steckler, and A. Lerner-Lam (2009). Migration imaging and forward modeling of microseismic noise sources near southern Italy. *Geochemistry, Geophysics, Geosystems*; doi:10.1029/2008GC002234.

Carpenter, M. A., R. J. Hemley, and H.-K. Mao (2000). High-pressure elasticity of stishovite and the P4(2)/mnm↔Pnnm phase transition. *Journal of Geophysical Research* **105**, 10,807–10,816.

Cassidy, J. F. (1992). Numerical experiment in broadband receiver function analysis. *Bulletin of the Seismological Society of America* **82**, 1,453–1,474.

Clowes, R. M., M. J. A. Burianyk, A. R. Gorman, and E. R. Kanasewich (2002). Crustal velocity structure from SAREX, the Southern Alberta Refraction Experiment. *Canadian Journal of Earth Sciences* **39**, 351–373.

Cook, F. A. (1995). The reflection Moho beneath the southern Canadian Cordillera. *Canadian Journal of Earth Sciences* **32**, 1,520–1,530.

Cook, F. A. (2002). Fine structure of the continental reflection Moho. *Geological Society of America Bulletin* **114**, 64–79; doi:10.1130/0016-7606.

Cook, F. A., D. J. White, A. G. Jones, D. W. S. Eaton, J. Hall, and R. M. Clowes (2010). How the crust meets the mantle: Lithoprobe perspectives on the Mohorovičić discontinuity and crust–mantle transition. *Canadian Journal of Earth Sciences* **47**, 315–351; doi:10.1139/E09-076.

Courtier, A. M., J. B. Gaherty, J. Revenaugh, M. G. Bostock, and E. J. Garnero (2010). Seismic anisotropy associated with continental lithosphere accretion beneath the CANOE array, northwestern Canada. *Geology* **38**, 887–890; doi:10.1130/G31120.1.

Dziewonski, A. M., and D. Anderson (1981). Preliminary reference earth model. *Physics of the Earth and Planetary Interiors* **25**, 297–356.

Dziewonski, A. M., and F. Gilbert (1976). The effect of small, aspherical perturbations on travel times and a re-examination of the corrections for ellipticity. *Geophysical Journal of Astronomical Society* **44**, 7–17.

Eaton, D. W., G. M. Ross, and R. M. Clowes (1999). Seismic reflection and potential-field studies of the Vulcan structure, western Canada: A Paleoproterozoic Pyrenees? *Journal of Geophysical Research* **104**, 255–269.

Eaton, D. W., G. M. Ross, F. A. Cook, and A. van der Velden (2000). Seismic imaging of the upper mantle beneath the Rocky Mountain foreland, southwestern Alberta. *Canadian Journal of Earth Sciences*, **37**, 1,493–1,507.

Efron, B., and R. Tibshirani (1991). Statistical data analysis in the computer age. *Science* **253**, 390–395.

English, J. M., and S. T. Johnson (2004). The Laramide orogeny: What were the driving forces? *International Geology Review* **46**, 833–838.

Fischer, K. M. (2002). Waning buoyancy in the crustal roots of old mountains. *Nature* **417**, 933–835.

Fouch, M. J., K. M. Fischer, M. E. Wysession, and T. J. Clarke (2000). Shear wave splitting, continental keels, and patterns of mantle flow. *Journal of Geophysical Research* **105**, 6,255–6,276.

Gaherty, J., and T. H. Jordan (1995). Lehmann discontinuity as the base of an anisotropic layer beneath continents. *Science* **268**, 1,468–1,471.

Gorman, A. R., R. M. Clowes, R. M. Ellis, T. J. Henstock, G. D. Spence, G. R. Keller, A. R. Levander, C. M. Snelson, M. J. A. Burianyk, E. R. Kanasewich, I. Asudeh, Z. Hajnal, and K. C. Miller (2002). Deep Probe—Imaging the roots of western North America. *Canadian Journal of Earth Sciences* **39**, 375–398.

Gu, Y. J., ed. (2010). *Arrays and Array Methods in Global Seismology*. Dordrecht, Netherlands: Springer, 274 pp.

Gu, Y. J., C. Dublanko, A. Lerner-Lam, K. Brzak, and M. Steckler (2007). Probing the sources of ambient seismic noise near the coasts of southern Italy. *Geophysical Research Letters* **34**, L22315; doi:10.1029/2007GL031967.

Gu, Y. J., K. Kocon, and A. Okeler (2009). Mapping the western boundary of the North American continent. American Geophysical Union Fall Meeting 2009, abstract DI41B-1807.

Gurrola, H., J. B. Minster, and T. Owens (1994). The use of velocity spectrum for stacking receiver functions and imaging upper mantle discontinuities. *Geophysical Journal International* **117**, 427–440.

Helmstaedt, H., and D. J. Schulze (1989). Southern African kimberlites and their mantle sample: Implications for Archaean tectonics and lithosphere evolution. In *Kimberlites and Related Rocks. Vol. 1. Their Composition, Occurrence, Origin, and Emplacement,* ed. J. Ross, 358–368. Proceedings of the Fourth International Kimberlite Conference, Perth, Australia. Carlton, Victoria [Australia]: Published for the Geological Society of Australia by Blackwell Scientific.

Hoffman, P. F. (1988). United plates of America, the birth of a craton: Early Proterozoic assembly and growth of Laurentia. *Annual Review of Earth and Planetary Sciences* **16**, 543–603.

Hyndman, R. D., C. A. Currie, and S. P. Mazzotti (2005). Subduction zone backarcs, mobile belts, and orogenic heat. *GSA Today* **15**, 4–10.

Hynes, A., and D. B. Snyder (1995). Deep-crustal mineral assemblages and potential for crustal rocks below the Moho in the Scottish Caledonides. *Geophysical Journal International* **123**, 323–339.

Kennett, B. L. N., M. Sambridge, and P. R. Williamson (1988). Subspace methods for large scale inverse problems involving multiple parameter classes. *Geophysical Journal International* **94**, 237–247.

Langston, C. A. (1979). Structure under Mount Rainier, Washington, inferred from teleseismic body waves. *Journal of Geophysical Research* **84**, 4,749–4,762.

Lemieux, S., G. M. Ross, and F. A. Cook (2000). Crustal geometry and tectonic evolution of the Archean crystalline basement beneath the southern Alberta Plains, from new seismic reflection and potential field studies. *Canadian Journal of Earth Sciences* **37,** 1,473–1,491.

Levander, A., and M. S. Miller (2010). The Moho and the lithosphere-asthenosphere boundary in the western U.S. Levin, V., and J. Park (1997). P-SH conversions in a flat-layered medium with anisotropy of arbitrary orientation. *Geophysical Journal International* **131**, 253–266.

Liu, L., M. Gurnis, M. Seton, J. Saleeby, R. D. Mueller, and J. M. Jackson (2010). The role of oceanic plateau subduction in the Laramide orogeny. *Nature Geoscience* **3**, 353–357.

Livaccari, R. F., K. Burke, and A. M. Sengor (1981). Was the Laramide orogeny related to subduction of an oceanic plateau? *Nature* **289**, 276–278.

Long, M. D., and P. G. Silver (2009). Shear wave splitting and mantle anisotropy: Measurements, interpretations, and new directions. *Surveys in Geophysics* **30**, 407–461.

Longuet-Higgins, M. S. (1950). A theory on the origin of microseisms. *Philosophical Transactions of the Royal Society of London* **243**, 1–35.

Mahan, K. H., and M. L. Williams (2005). Reconstruction of a large deep-crustal terrane: Implications for the Snowbird tectonic zone and early growth of Laurentia. *Geology* **33**, 385–388; doi:10.1130/G27273.1.

Mangino, S., and K. Priestley (1998). The crustal structure of the southern Caspian region. *Geophysical Journal International* **133**, 630–648.

Marone, F., and B. Romanowicz (2007). On the depth distribution of azimuthal anisotropy in the continental upper mantle. *Nature* **447**, 198–201.

Maxson, J., and B. Tickoff (1996). Hit-and-run collision model for the Laramide orogeny, western United States. *Geology* **24**, 968–972; doi:10.1130/0091-7613(1996)024.

Menke, W., and V. Levin (2003). The cross-convolution method for interpreting *SKS* splitting observations, with application to one and two layer anisotropic Earth models. *Geophysical Journal International* **15**, 379–392.

Mercier, J.-P., M. G. Bostock, J. F. Cassidy, K. Dueker, J. B. Gaherty, E. J. Garnero, J. Revenaugh, and G. Zandt (2009) Body-wave tomography of western Canada. *Tectonophysics* **475**, 480–492; doi:10.1016/j.tecto.2009.05.030.

Mueller, P. A., A. L. Heatherington, D. M. Kelly, J. L. Wooden, and D. W. Mogk (2001). Paleoproterozoic crust within the Great Falls tectonic zone: Implications for the assembly of southern Laurentia. *Geology* **30**, 127–130; doi:10.1130/0091-7613.

Nettles, M., and A. M. Dziewonski (2008). Radially anisotropic shear-velocity structure of the upper mantle globally and beneath North America. *Journal of Geophysical Research* **113**, B02303; doi:10.1029/2006JB004819.

Park, J., and V. Levin (2000). Receiver functions from multiple-taper spectral correlation estimates. *Bulletin of the Seismological Society of America* **90**, 1,507–1,520; doi:10.1785/0119990122.

Price, R. A. (1981). The Cordilleran foreland thrust and foldbelt in the Southern Canadian Rocky Mountains. In McClay, K. R., and N. J. Price (eds.) *Thrust and Nappe Tectonics. Special Publication of the Geological Society of London* **9**, 427–448.

Rawlinson, N., and M. Sambridge (2005). The fast marching method: An effective tool for tomographic imaging and tracking multiple phases in complex layered media. *Exploration Geophysics* **36**, 341–350.

Rondenay, S. (2009). Upper mantle imaging with array recordings of converted and scattered teleseismic waves. *Surveys in Geophysics* **4–5**, 377–405; doi:10.1007/s10712-009-9071-5.

Ross, G. M. (2000). Introduction to special issue of Canadian Journal of Earth Sciences: the Alberta Basement Transect of Lithoprobe. *Canadian Journal of Earth Sciences* **37**, 1,447–1,452.

Ross, G. M., and D. W. Eaton (2002). Proterozoic tectonic accretion and growth of western Laurentia: Results from Lithoprobe studies in northern Alberta. *Canadian Journal of Earth Sciences* **39**, 313–329; doi:10.1139/E01-081.

Ross, G. M., D. W. Eaton, D. E. Boerner, and W. Miles (2000). Tectonic entrapment and its role in the evolution of continental lithosphere: An example from the Precambrian of western Canada. *Tectonics* **19**, 116–134.

Ross, G. M., R. R. Parrish, M. E. Villeneuve, and S. A. Bowring (1991). Geophysics and geochronology of the crystalline basement of the Alberta Basin, western Canada. *Canadian Journal of Earth Sciences* **28**, 512–522.

Shapiro, N. M., M. Campillo, L. Stehly, and M. H. Ritzwoller (2005). High resolution surface wave tomography from ambient seismic noise. *Science* **307**, 1,615–1,618.

Sheehan, A. F., G. A. Abets, C. H. Jones, and A. L. Lerner-Lam (1995). Crustal thickness variations across the Colorado Rocky Mountains from teleseismic receiver functions. *Journal of Geophysical Research* **100**, 20,391–20,404.

Shragge, J., M. G. Bostock, and R. M. Ellis (2002). Integrated teleseismic studies of the southern Alberta upper mantle. *Canadian Journal of Earth Sciences* **39**, 399–411.

Silver, P. G., and W. W. Chan (1991). Shear wave splitting and subcontinental mantle deformation. *Journal of Geophysical Research* **96**, 16,429–16,454.

van der Lee, S., and A. Frederiksen (2005). Surface wave tomography applied to the North American upper mantle. In *Seismic Earth: Array Analysis of Broadband Seismograms*, ed. A. Levander and G. Nolet, 67–80. Washington, DC: American Geophysical Union.

Vinnik, L. (1977). Detection of waves converted from *P* to *SV* in the mantle. *Physics of the Earth and Planetary Interiors* **15**, 39–45.

Weaver, R. L. (2005). Information from seismic noise. *Science* **307**, 1,568–1,569.

Welford, J. K., and R. M. Clowes (2004). Deep 3-D seismic reflection imaging of Precambrian sills in southwestern Alberta, Canada. *Tectonophysics* **388**, 161–172.

Yang, X., Y. J. Gu, P. Shen, X. Liu, and Z. Zheng (2006). A study of the adaptive method for decoupling overlapped seismic records. *Pure and Applied Geophysics* **163**, 1,515–1,536.

Yang, Y., and M. Ritzwoller (2008). Characteristics of ambient seismic noise as a source for surface wave tomography. *Geochemistry, Geophysics, Geosystems* **9**, Q02008; doi:10.1029/2007GC001814.

Yang, Y., M. H. Ritzwoller, and C. H. Jones (2011). Crustal structure determined from ambient noise tomography near the magmatic center of Coso region, southeastern California. *Geophysics, Geochemistry, Geosystems* **12**, Q02009; doi10.1029/2010GC003362.

Yang, Y., M. H. Ritzwoller, A. L. Levshi, and N. M. Shapiro (2006). Ambient noise Rayleigh wave tomography across Europe. *Geophysical Journal International* **168**, 259–274.

Yao, H., R. D. van der Hilst, and M. V. De Hoop (2006). Surface-wave array tomography in SE Tibet from ambient seismic noise and two-station analysis: I—Phase velocity maps. *Geophysical Journal International* **166**, 732–744.

Yuan, H., and B. Romanowicz (2010). Lithospheric layering in the North American craton. *Nature* **466**, 1,063–1,068.

Zelt, B. C., and R. M. Ellis (1999). Receiver-function studies in the Trans-Hudson orogen, Saskatchewan. *Canadian Journal of Earth Sciences* **36**, 585–603.

Zhu, L., and H. Kanamori (2000). Moho depth variation in southern California from teleseismic receiver functions. *Journal of Geophysical Research* **105**, 2,969–2,980.

***Department of Physics***
***University of Alberta***
***Edmonton, Alberta T6G2G7 Canada***
***ygu@ualberta.ca***
***(Y. J. G.)***